



LJMU Research Online

Ehtezazi, T

SARS-CoV-2: characterisation and mitigation of risks associated with aerosol generating procedures in dental practices (Feb, 10.1038/s41415-020-2504-8, 2021)

<http://researchonline.ljmu.ac.uk/id/eprint/14500/>

Article

Citation (please note it is advisable to refer to the publisher's version if you intend to cite from this work)

Ehtezazi, T (2021) SARS-CoV-2: characterisation and mitigation of risks associated with aerosol generating procedures in dental practices (Feb, 10.1038/s41415-020-2504-8, 2021). BRITISH DENTAL JOURNAL. ISSN 0007-0610

LJMU has developed **LJMU Research Online** for users to access the research output of the University more effectively. Copyright © and Moral Rights for the papers on this site are retained by the individual authors and/or other copyright owners. Users may download and/or print one copy of any article(s) in LJMU Research Online to facilitate their private study or for non-commercial research. You may not engage in further distribution of the material or use it for any profit-making activities or any commercial gain.

The version presented here may differ from the published version or from the version of the record. Please see the repository URL above for details on accessing the published version and note that access may require a subscription.

For more information please contact researchonline@ljmu.ac.uk

<http://researchonline.ljmu.ac.uk/>

SARS-CoV-2: Characterisation and Mitigation of Risks Associated with Aerosol Generating Procedures (AGPs) in Dental Practices

Touraj Ehtezazi¹, David G Evans¹, Ian D Jenkinson*^{1, 2}, VJ Vadgama³, Jaimini Vadgama³, Fadi Jarad⁴, Nicholas Grey⁵, Robert P Chilcott⁶

¹Liverpool John Moores University, James Parsons Building, Byrom Street, Liverpool, L3 3AF

²Techceram Limited, 9b Sapper Jordan Rossi Park, Baildon, Shipley, BD17 7AX

³Woodbury Dental & Laser Clinic, Woodbury House, 149 High Street, Tenterden, Kent, TN30 6JS

⁴University of Liverpool School of Dentistry, Research Wing, Pembroke Place, L3 5PS

⁵University of Manchester School of Dentistry, Coupland 3 Building, Oxford Road, M13 9PL

⁶University of Hertfordshire, College Lane, Hatfield, Hertfordshire, AL10 9AB

* Correspondence to: Prof Jenkinson Email: I.D.Jenkinson@ljmu.ac.uk

Key Points

1. The particle size distribution of aerosols generated by dental procedures are predominantly < 0.3 µm in diameter. This encompasses the reported size range of the SARS-CoV-2 virus (0.05 – 0.15 µm).
2. Even in the presence of interventions such as high volume inter-oral suction HVS(IO) combined with an air cleaning system (ACS), aerosol particles < 0.3 µm were substantially elevated above the baseline range during the dental aerosol generating procedures (AGP) used in this study (these included the use of air-turbine and electric handpieces operating at over 60,000 rpm). Levels of aerosol were especially elevated within the working micro-environment (50 cm radius from the mouth) of the dentist and assistant. This emphasises the importance of properly fitted personal protective equipment such as FFP3 masks.
3. Intra-oral high-volume suction, either alone or in combination with an air cleaning system (in this case operating at 24 room air changes per hour in a typical 35 m³ surgery) was effective in rapidly reducing AGP-related particle concentrations to within background range in some cases, during or immediately, on cessation of AGPs negating the need for fallow time. These data indicate that a reduction in fallow time may be achieved below the current guidance of 10 minutes through judicious use of aerosol management interventions.

Abstract

The objectives of this study were to characterise the particle size distribution of aerosols generated by standard dental aerosol generating procedures (AGPs) and to assess the impact of aerosol management interventions on 'fallow time'. Aerosol management interventions included combinations of high-volume intra-oral suction (HVS(IO)), high volume extra-oral suction (HVS(EO)) and an air cleaning system (ACS). A sequence of six AGPs were performed in succession on a phantom head. Real-time aerosol measurements (size range 0.0062 – 9.6 μm) were taken using a high-resolution particle sizer acquiring air samples from six locations within a typical dental treatment room (35 m^3). The majority (>99%) of AGP particles were < 0.3 μm diameter and remained at significant levels around the dental team during the AGPs. This emphasises the importance of personal protection equipment, particularly, the use of properly fitted respiratory protection to the appropriate (FFP3) standard. In the absence of active aerosol management interventions, AGP particles were estimated to remain above the baseline range for around 25-31 minutes from the end of the sequence of procedures. It was found that HVS(IO), either alone or in combination with the ACS, reduced particle concentrations to baseline levels on completion of AGPs. Overall, these data indicate that there is scope to eliminate fallow time. However, it should be noted that this study was performed using a phantom head and so confirmatory studies with patients are required.

Introduction

Potentially infectious agents (e.g. bacteria, fungi and viruses) can be transmitted when droplets containing microorganisms generated from an infected person (example by breathing, talking or coughing) are propelled through the air and are directly inhaled, deposited on the skin or mucosal surfaces, or contaminate infrastructure.¹ High-speed dental instruments require effective cooling of the work area in order to avoid damage of the pulp dentine system. These instruments generate a dental aerosol, as cooling water and air are sprayed around the instruments and the oral cavity.

Dental aerosols are distributions of particle sizes from 0.001 to >10 µm in diameter.^{2,3} Traditionally, dental airborne aerosols were defined as being small particles <50 µm, with larger ballistic/projectile particles (>50 -100 µm) being described as “splatter”.⁴ The WHO definition⁵ of aerosols has been adopted in the dental field, which defines large projectile particles as being > 5µm, with smaller (< 5 µm) “droplet nuclei” particles forming through the evaporation of larger particles generating an airborne solid residue.

Infectious droplets from saliva or blood may enter the aerosol and expose the dental team to an increased risk of infection through direct inhalation, contact with eyes, and contact with contaminated work surfaces.^{6,7} Dental aerosols therefore have the potential to provide a path for the transmission of COVID-19^{8,9} which may remain infectious for between 2 hours to 9 days in a humid environment.⁷ Research on the influenza virus has also demonstrated that the total viral copies were 8.8 times more numerous in particles <5 µm than in particles ≥5 µm.¹⁰ Previous studies have demonstrated the dispersion of bioaerosols to all areas of the treatment room¹¹ which remain airborne for 30 minutes following the procedure.¹² Therefore, there is a clear need for the effective removal of aerosols in dental practices.¹³

Protocols exist to minimise the risk of infection to clinical staff during dental procedures.^{12,14-17} These include: low volume suction (LVS) to remove saliva and excess coolant, coolant disinfectant, high-volume intra-oral suction (HVS (IO)), personal protective equipment (PPE) and improved ergonomics and techniques (e.g. dental dams). A range of additional aerosol removal treatments have been proposed for use in dental procedures including extra-oral high volume suction (HVS (EO)), air cleaning systems (ACS), designed to filter, purify and recirculate room air) and ventilation systems.^{7,14,18,19} However, their effectiveness within a diverse range of dental practice environments is difficult to predict.¹³

A wide range of ACS with different air flow rates and cleaning technology are commercially available or being marketed for dental use. However, dental practices have no clear standards or specifications to refer to before making an investment. HVS(EO) and ACS^{20,21} that contain high efficiency particulate air (HEPA) filters are effective in removing airborne particles with sizes greater than 0.3 µm: viruses, such as coronaviruses, are in the size range of 0.05 – 0.15µm²² and thus may evade filtration. Hence, ACS have evolved to include the addition of technology such as UV-C lamps (99.97% killing of H3N2 influenza virus), negative ion generators, and high pressure/voltage electrostatic plasma, which eliminate particles greater than 0.0146 µm. The efficiency of these air purifiers has not been evaluated for the removal aerosol particles in the presence of high volume intra-oral or extra-oral suction.

Whilst researchers have studied aerosol removal treatments, few studies have examined their effectiveness across the full dental aerosol particle size distribution. For example, the use of HVS(IO) at air flow rates of 250 – 300 L min⁻¹ is an established means of controlling dental aerosols but its effectiveness is based on a qualitative assessment of visible particles or particles greater than 0.65 µm.^{19,23} Viruses are smaller than 0.65 µm and therefore the efficacy of HVS(IO) studies are not relevant to COVID 19.

The objectives of this current study were to characterise the aerosols generated by standard dental procedures and to investigate the effectiveness of different combinations aerosol management interventions across the particle distribution range from 0.0062 to 10 µm diameter to provide evidence for establishing a revised fallow time. A sequence of six standard dental procedures were performed in series to assess the effectiveness of four combinations of interventions based on HVS (IO), HVS (EO) and an ACS. The effectiveness of each intervention group was measured using a high-resolution particle size analyser, with air samples taken over a 36-minute period from six locations within a standard dental surgery.

Materials and Method

The study was performed within a dental surgery (dimensions 4.4 x 3.1 x 2.6 m: Figure 1). All non-experimental air-conditioning equipment was turned off during the experimental work, and the average room temperature and relative humidity over the study period were 27° C and 67%, respectively.

A phantom head (Simple Manikin III, Phantom Head Dental, UK) was used as a patient surrogate containing a Kilgore Nissin 200 series typodont (containing melamine teeth) with SPMIII oral cavity cover.

Real-time aerosol analysis was performed with a high-resolution Electric Low-Pressure Impactor particle sizer (HR-ELPI: “ELPI+”, Dekati, Kangasala, Finland). The instrument recorded the concentration of particles detected within 100 pre-set ‘bins’ of particle size, ranging from 0.0062 to 9.6 µm, at a sampling frequency of 1 Hz. Air samples were acquired at six locations (Figure 1, Table S1). Each position was measured relative to the phantom head on which the dental AGPs were performed. Air samples were directed to the ELPI+ via 2 m lengths of silicone tubing (Tygon[®]; internal diameter 12.7 mm, external diameter 17.5 mm; Cole-Parmer Instrument Co, Illinois, USA: Figure S1). Each tube was individually connected to the particle sizer for a period of 30 seconds before being replaced with a tube from the next sampling location to enable a serial analysis of all six air sample locations within a 3 min cycle. The initial 5 seconds of data acquisition was ignored to allow for purging of the sample air lines. A pilot study demonstrated that the tubing had no discernible effect on particle size measurements (see supplementary data: Annex A, Figures S1-S3).

Each experiment comprised a three-minute baseline period, followed by a series of six, three-minute aerosol generating procedures (AGPs), giving a total procedural duration of 18 minutes with a post-procedural duration of 15 minutes to monitor aerosol decay (Figure 2). Each experiment was performed under one of four treatments conditions (Table S2) performed in triplicate. The specifications of each aerosol removal system are described in

Table 1. The AGPs incorporated the serial use of six commonly used dental preparation instruments, each of which were operated for three minutes within the phantom head in the upper and lower anterior sextants in the following order: (I) Air turbine handpiece, (II) Electric contra-angle handpiece, (III) Air turbine handpiece, (IV) Three in one syringe, (V) Ultrasonic scaler and (VI) Ultrasonic scaler (Table S3). There was no delay between the use of each handpiece. Each procedure was performed on separate teeth in a predefined sequence: (I) upper left quadrant (from tooth 18 – 14), (II) upper anterior quadrant (13 – 23), (III) upper right quadrant (24 – 28), (IV) lower left quadrant (38 – 34), (V) lower anterior quadrant (33 – 43) and (VI) lower right quadrant (44 – 48). The ultrasonic procedures (V and VI) were performed at the gingival margin.

Total particle concentration (calculated as the sum of particle concentrations over the 0.0062 to 9.6 μm bin range) did not consistently exhibit a Gaussian (normal) or log-normal distribution and so excluded the use of parametric statistical tests. The low sample number ($n=3$) precluded non-parametric analyses. Therefore, descriptive statistics were used and all particle concentration data are expressed as median values. Area under curve (AUC) calculations were performed using GraphPad Prism (v7.0e for Mac OS, GraphPad Software, La Jolla California USA). The AUC calculations reflect the total “dose” of aerosol (units of $\text{mL cm}^{-3} \text{ min}$). The AUC calculations were used to assess the overall efficiency of each treatment and were expressed as the median value \pm minimum/maximum. Estimation of fallow time in the control treatment group was performed by linear regression of particle concentrations at each sample location following cessation of AGPs and was calculated as the time at which the extrapolated particle concentration decreased below the upper baseline particle concentration.

Results

The majority (>99.9%) of particles generated by the sequence of dental procedures were < 0.3 μm diameter when sampled at the proximal position (Location 1: 8 cm). Instruments I, II and III (Table S3) in the sequence generated the highest aerosol levels. Peak concentrations occurred between particle diameters 0.013 to 0.022 μm (Figure 3, $t= 3\text{-}6, 6\text{-}9, \text{ and } 9\text{-}12 \text{ min}$).

Aerosol generated under the control conditions (Table S2, intervention group A (LVS only)) was observed at all locations within the surgery and remained detectable at 15 min (Figure 3, $t=36 \text{ min}$) from the end of the last procedure (instrument VI at $t=21 \text{ min}$). The most persistent particles were in the range 0.012 to 0.025 μm . Particle concentrations decreased with increasing distance from the phantom head, with a notable, time-related decrease of particles in the range 0.054 to 0.236 μm diameter. Particles > 0.05 μm persisted at low concentrations ($\sim 25 \times 10^3 \text{ cm}^{-3}$) for the duration of the study.

The particle size distributions generated during the use of all instruments and applying interventions B to E (Table S2) were like those in the control but with markedly reduced concentrations (Figure 3). Compared with control conditions all interventions produced a remarkable decrease in the number and distribution of particles detected in the extra-oral space (Location 2: 20 cm) and more distal locations. Following the end of the sequence of procedures ($t=21 \text{ min}$) there was infrequent detection of low concentrations of aerosol

particles from beyond the extra-oral space, and particles $> 0.05 \mu\text{m}$ were generally at the baseline level (Figure 3).

In the control group, total particle counts remained elevated above the baseline range for the duration of the experiment at all locations (Figure 4, and Figure S4). Therefore, for the control group linear regression was used to calculate the time needed for the total particle concentration at each location to return to baseline levels (Figure S10). This produced an estimated median time of 26 min (range 25 – 31 min) from the end of the sequence of procedures ($t=21$ min). In the case of experiments using either the HVS(IO), or the HVS(IO) combined with the ACS (Table S2; intervention groups B and C) the concentration of particles returned to within the baseline range at the end of the procedures ($t=21$ min) (Figures S7 and S8 respectively). However, the total number of aerosol particles remained marginally above the baseline for interventions which included the HVS(EO) (Figures S9 and 5).

When the aerosol concentrations are expressed as dose ($\text{mL cm}^{-3} \text{ min}$) all interventions reduced total aerosol exposure (Figure 6). Intervention group B (Table S2; HVS(IO) with LVS) reduced the median dose by 80%, while intervention group E (HVS(IO)+HVS(EO)+ACS with LVS) reduced the median dose by 90%. However, HVS(IO) was noticeably less effective than intervention groups C, D and E in controlling the range of (maximum-minimum) of the dose. A pictorial summary of these data is provided in Figure S6.

Discussion

The results of this study demonstrate that all the aerosol management interventions evaluated were relatively effective in controlling aerosols generated by dental handpieces. Most particles produced by our sequence of AGPs were $< 0.3 \mu\text{m}$. The use of either the HVS(IO), or the HVS(IO) combined with the ACS was enough to reduce the fallow time to 0-min. . Please refer to Figure 2 for fallow time and Figure 3 for zero fallow time, right of the superimposed black vertical 18–21-minute lines.

During AGPs the concentration of particles in the range 0.05 to $0.15 \mu\text{m}$ diameter range is increased substantially. This size range corresponds to the reported size range of the SARS-CoV2 virus (0.05 to $0.15 \mu\text{m}$).²² Within the working micro-environment (Locations 3-4, <50 cm) the presence of active aerosol management interventions substantially reduces the concentration of airborne particles in this range but does not eliminate them. Thus it is important for dental workers to utilise both appropriate and properly fitted respiratory protective equipment such as FFP3 masks in combination with aerosol management interventions.²⁴

In the absence of aerosol management interventions, particles in the range 0.05 – $0.236 \mu\text{m}$, remained at elevated concentrations within the macro-environment (Locations 5-6, >50 cm) for longer than the experimental period. Our control study estimated that it may take at least 28 to 34 minutes after cessation of AGPs for the total particle concentration to return to baseline levels. Intervention groups B and C, which included the addition of HVS(IO), or HVS(IO) with ACS, both had the effect of returning particle concentrations to within the baseline range by the end of the sequence of procedures i.e. no additional fallow-time was required before particle concentrations returned to baseline levels. In the case of

interventions D and E, which included HVS(EO), particle concentrations remained marginally above the baseline which is in agreement with previous work.¹⁹

Interventions B and C reduced particle concentrations in the macro-environment (Locations - 5-6, >50 cm) to within the baseline range during AGPs. Intervention C, (HVS(IO) in combination with an ACS) was effective in controlling both the median and the range (max-min) of the aerosol dose at all locations. In a dental surgery of the size used in this study (35 m³), and in the context of SARS-CoV-2, it provides further evidence to support a reduction in fallow time below the current recommend period of 10 minutes²⁴ in agreement with other recent studies.²⁵

The use of a phantom head is a clear limitation of this study: the **absence** of saliva and other biological materials within the oral cavity may conceivably have influenced the particle size distribution of the aerosols. The standard procedures used in this study used aqueous coolant (Table S3) which, under normal circumstances, would have led to a large (25 to 82-fold) dilution in patient-generated saliva. Thus, the impact of omitting salivary fluid on aerosol particle size range would likely be minimal. However, it is clear that further, confirmatory research should be performed using patients. Such work should incorporate different size surgeries to validate the scalability of aerosol mitigation interventions. It should also be noted that a locally moist and warm atmosphere within a “turbulent gas cloud” allows the contained continuum of droplet sizes to evade evaporation for much longer time periods than occurs with isolated droplets, from a fraction of a second to minutes.²⁶ This may explain why the most persistent particles measured in our study were within the smaller, 0.012-0.025 µm range. Therefore, a patient-orientated study is needed to confirm the nature of the fine particle aerosols containing mixtures of saliva, coolant, and pathogens. This may provide further evidence to support the use of antiviral disinfectants in coolant solutions.

Conclusions

Dental AGPs produce aerosols characterised by particles < 0.3 µm in diameter. Although aerosol suppression treatments such as HVS(IO) alone or in combination with an ACS may rapidly reduce particle concentrations to within background range, they do not eliminate exposure during AGPs and so the use of appropriate respiratory protective equipment by dental practitioners is essential.

HVS(IO) combined with the ACS was enough to reduce the fallow time to 0 minute, and to control the median and range of the aerosol particle dose at all areas in the surgery. The ACS used in these experiments was set to deliver 24 air changes per hour in an 35m³ surgery which was close to maximum and further experimental work is needed to optimise the location and setting of equipment of this type.

In the absence of ventilation within a modest sized (35 m³) surgery, particles associated with dental AGPs may persist for approximately half an hour. There appears to be scope for a reduction in fallow time from the current guideline of 10 minutes when effective aerosol management system(s) are used.

Acknowledgements

This work was supported by the LJMU Corona Virus Rapid response grant. The authors wish to thank Tayyebah Rafiei, Rhiannon Powell & Ben Wilkinson for their efforts in assisting the data analysis. The authors would also like to express their gratitude to Louie Chen (Sciolutions Ltd) & Dekati Ltd Finland for the loan of the ELPI+ unit and their invaluable technical support.

Declaration of Interests

The authors have not declared any conflict of interest. Techceram Ltd is a commercial entity in the dental field, but has no interest in any of the equipment used in the present study, only in contributing its network of contacts towards the present study, in order to better understand dental AGPs, so that dental hospitals, practices, labs and associated dental supply chain smaller businesses can remain open and operate safely through any future viral pandemics.

Figure 1: Layout and sampling positions within the dental treatment room. Note that the tube at location 6 was moved from the ceiling light fitting to be visible in the photograph.

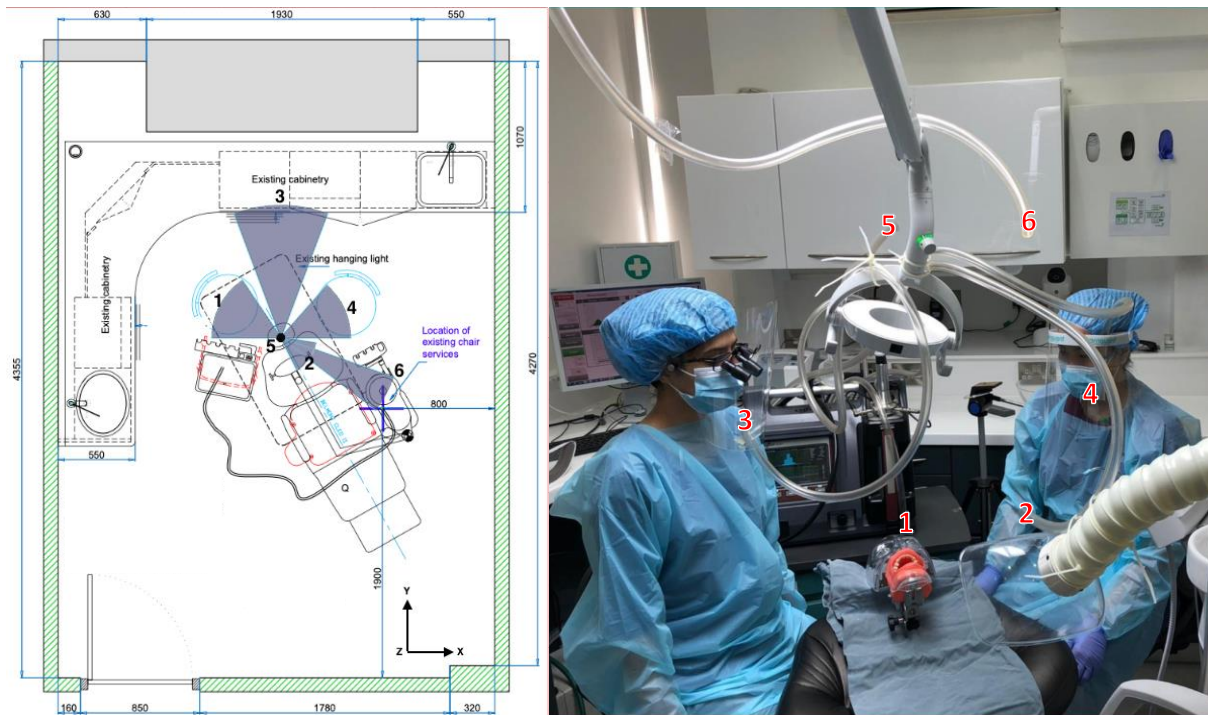


Figure 2: Outline study design. After an initial baseline period (3 min), six aerosol generating procedures (I to VI) were performed in series (18 min) followed by a period to quantify aerosol decay kinetics (15 min). Air samples from each location (1 – 6) were acquired over a 30 second period. The total duration of each experiment was 36 minutes.

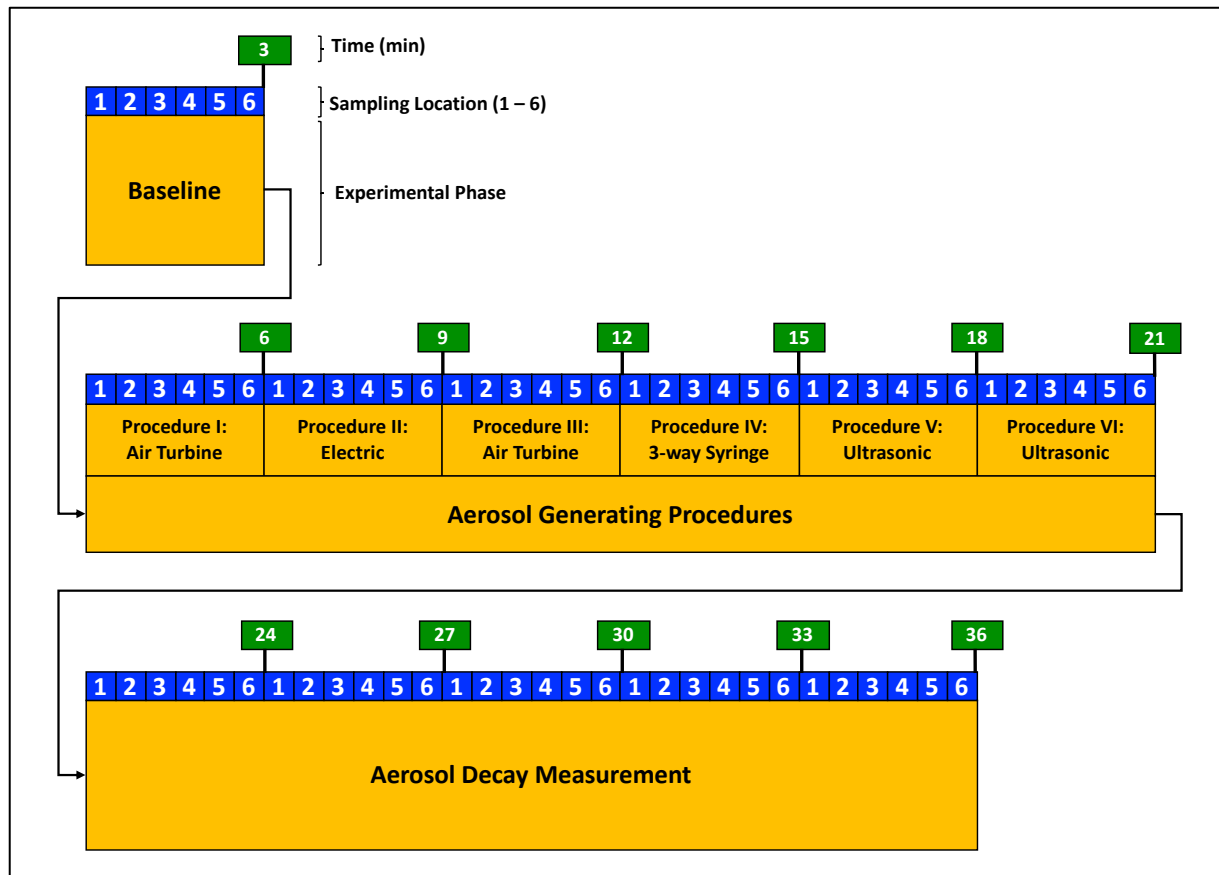


Figure 3: Temporal, spatial and size characterisation of particles generated during AGPs (measured by HR-ELPI) for each location (1 – 6; Table 1) and treatment group (A – E; Table 2). Acquisition of air samples were performed during the baseline period (0 – 3 min), during the six procedures (3 – 21 min) and following cessation of procedures (21 – 36 min). Each data point represents the median particle concentration per size bin ($\# \text{ cm}^{-3}$) derived from $n=3$ replicates. The dotted lines indicate the lower reported size for a SARS-CoV-2 virus particle (50 nm diameter).

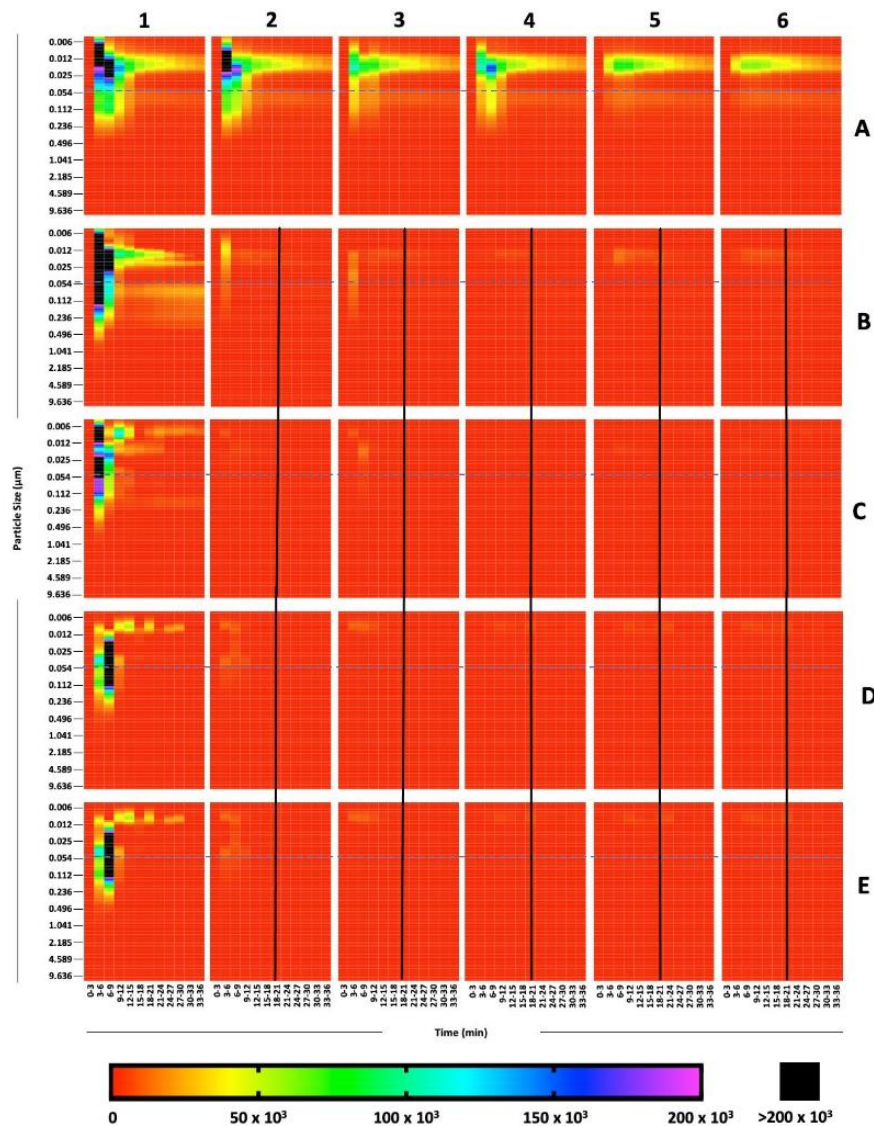


Figure 4: Total particle concentration generated during AGPs in the absence of interventions (treatment group A; Table 2) at each air sampling location (1 – 6; Table 1). Acquisition of air samples were performed during the baseline period (0 – 3 min), during the six procedures (3 – 18 min) and following cessation of procedures (18 – 36 min). Dotted lines indicate the upper and lower boundaries of the baseline data. Each data point represents the sum of particles measured by HR-ELPI over 1 second during each replicate ($n=3$).

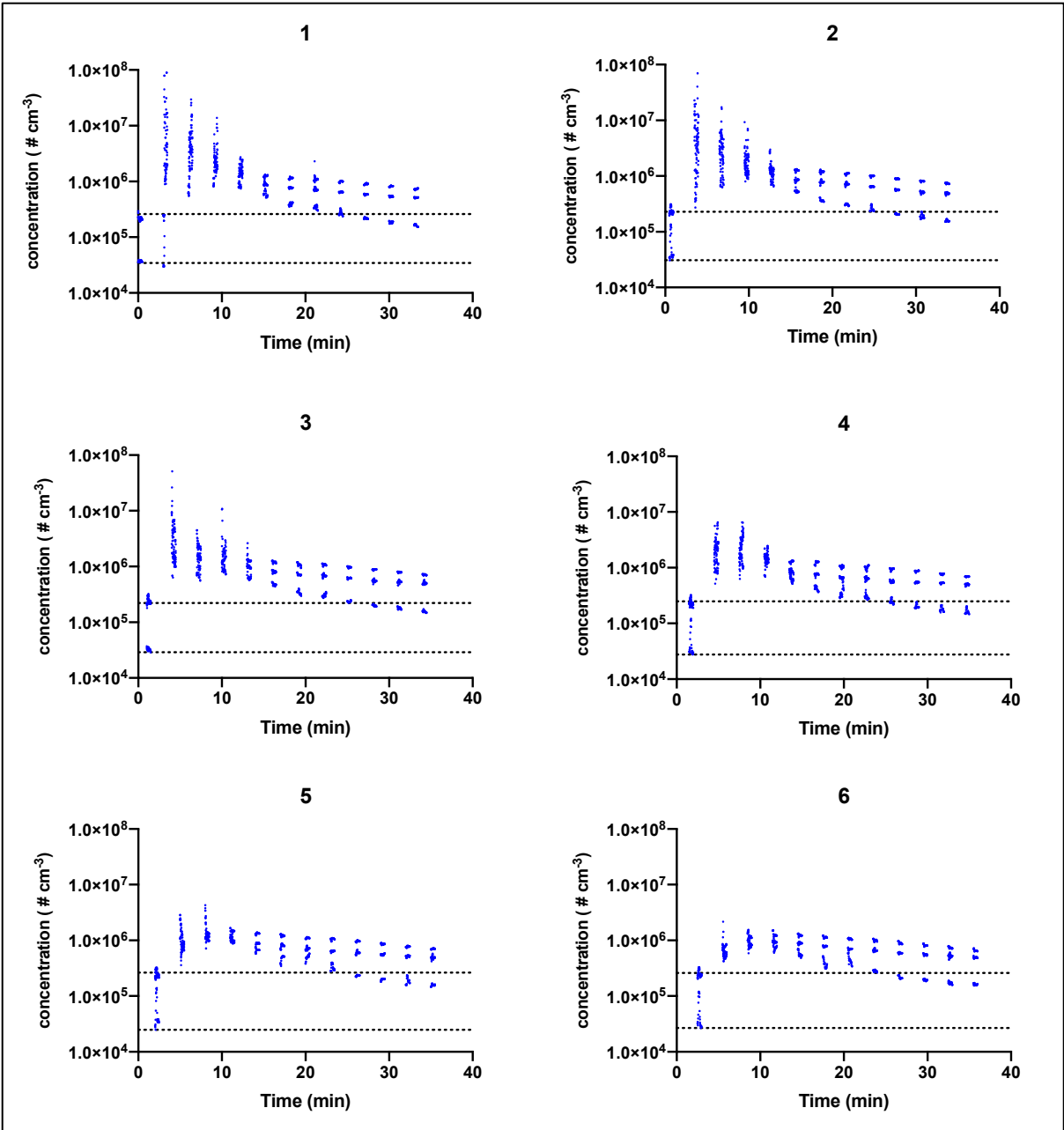


Figure 5: Total particle concentration generated during AGPs in the presence of HVS(IO), HVS(EO) and ACS (treatment group E; Table 2) at each air sampling location (1 – 6; Table 1). Acquisition of air samples were performed during the baseline period (0 – 3 min), during the six procedures (3 – 18 min) and following cessation of procedures (18 – 36 min). Dotted lines indicate the upper and lower boundaries of the baseline data. Each data point represents the sum of particles measured by HR-ELPI over 1 second during each replicate (n=3).

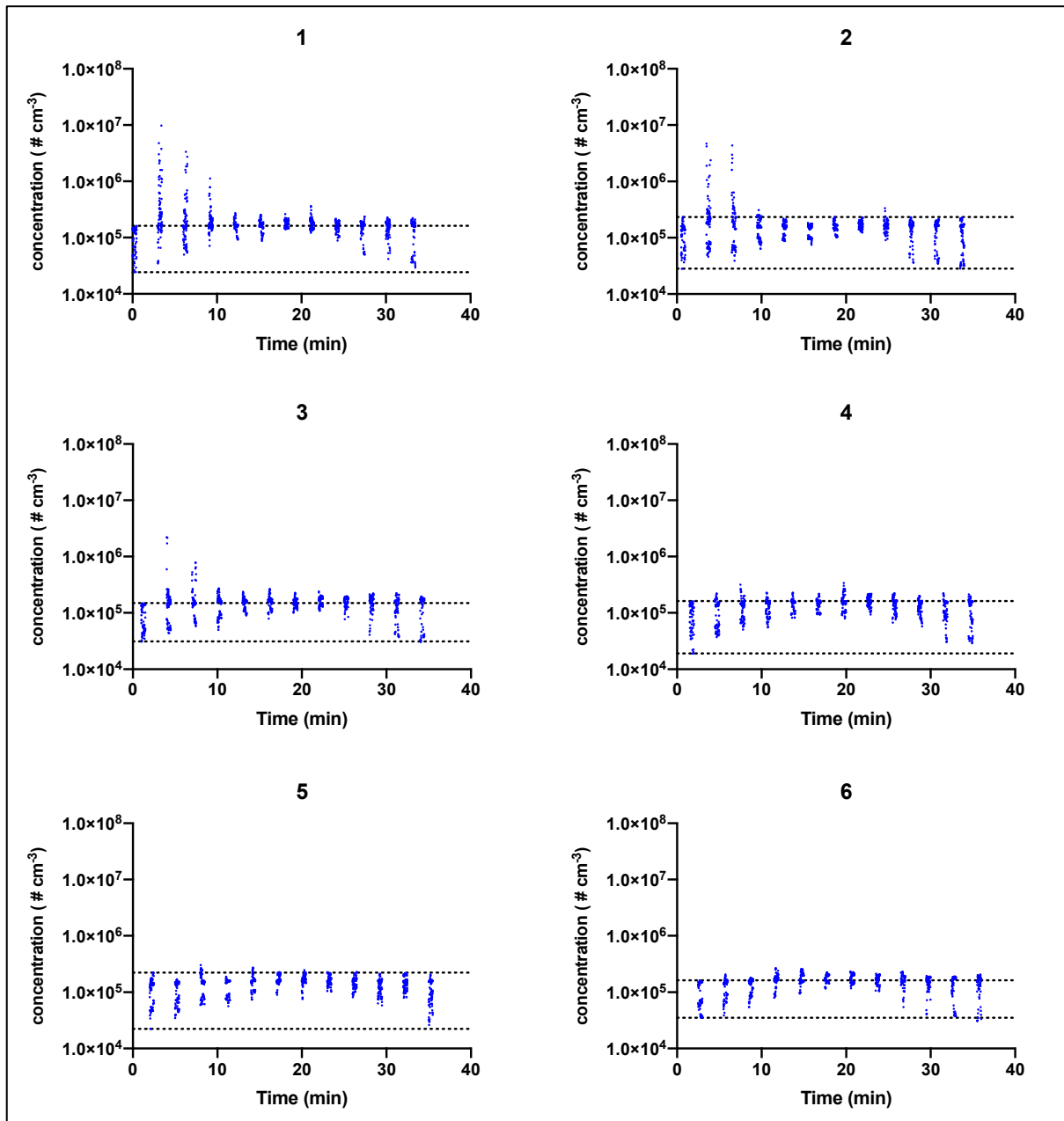


Figure 6: Total dose of particles measured over the 36 minute experimental period (expressed as area under curve) for each location (1 – 6; Table 1) and treatment group (A – E; Table 2). Each data point represents the median \pm minimum/maximum of n=3 replicates.

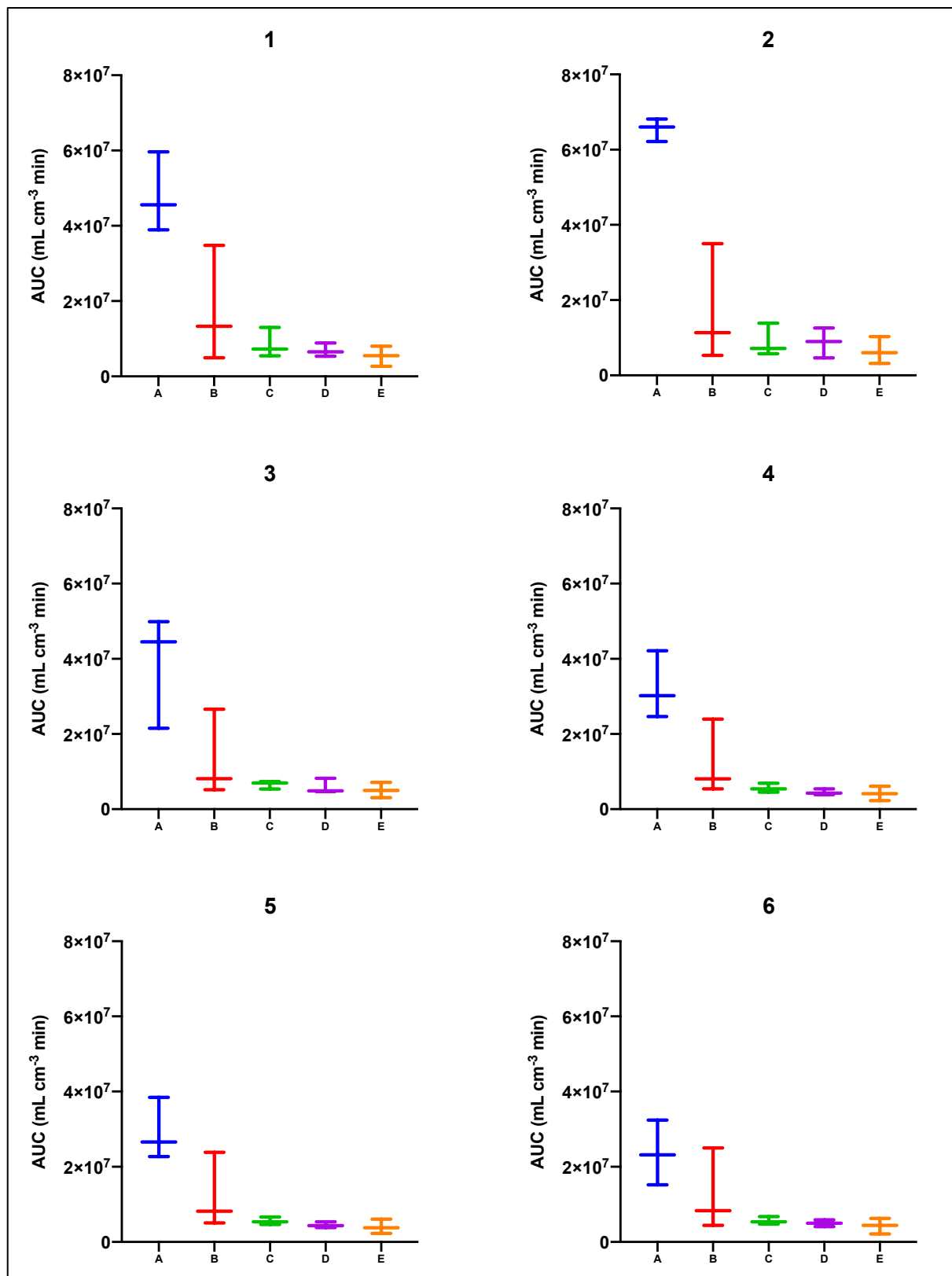


Table 1: Aerosol suppressing equipment and corresponding air/water flow rates. Low volume suction (LVS) was used in all treatment groups. In this study, the air cleaning system (ACS) flow rate was equivalent to ~ 24 air changes per hour. [§]The VacStation contains two H13 grade HEPA filters (lower particle size limit 0.3 µm) with a post-filter UVC light sterilisation stage. [†]The Q7 air cleaning system is a filter-less instrument which operates on a high voltage plasma purification process with integral ion chamber sterilisation stage; the lower particle size limit is reportedly 14.6 nm.

Treatment	Equipment	Water Flow (L min ⁻¹)	Air Flow (L min ⁻¹)	Air changes per hour (in a 35 m ³ surgery)
LVS	Plastcare USA, 4 mm slow speed salivary ejector.	2.4	79	
HVS(IO)	Dürr Universal Cannula III 16 mm, connected to Dürr Dental VSA 300S Dürr Dental UK, Kettering, UK.	-	297	
HVS(EO)	Eighteenth VacStation, Sifary Medical Technology, Jiangsu, China.	-	3700	6
ACS	Woodpecker Q7 Plasma Air Purifier, Guilin Woodpecker Medical Instrument Co, Guilin, China.	-	14167	24

References

- 1 Jayaweera, M., Perera, H., Gunawardana, B. & Manatunge, J. Transmission of COVID-19 virus by droplets and aerosols: A critical review on the unresolved dichotomy. *Environ Res* **188**, 109819, doi:10.1016/j.envres.2020.109819 (2020).
- 2 Bogdan, A., Buckett, M. I. & Japuntich, D. A. Nano-sized aerosol classification, collection and analysis--method development using dental composite materials. *J Occup Environ Hyg* **11**, 415-426, doi:10.1080/15459624.2013.875183 (2014).
- 3 Day, C. J., Price, R., Sandy, J. R. & Ireland, A. J. Inhalation of aerosols produced during the removal of fixed orthodontic appliances: a comparison of 4 enamel cleanup methods. *Am J Orthod Dentofacial Orthop* **133**, 11-17, doi:10.1016/j.ajodo.2006.01.049 (2008).
- 4 Micik, R. E., Miller, R. L., Mazzarella, M. A. & Ryge, G. Studies on dental aerobiology. I. Bacterial aerosols generated during dental procedures. *J Dent Res* **48**, 49-56, doi:10.1177/00220345690480012401 (1969).
- 5 Organisation, W. H. *Infection prevention and control of epidemic and pandemic prone respiratory infections in health care*. (WHO Library Cataloguing-in-Publication Data 2014).
- 6 Miller, R. Air Pollution in the Dental Office. *Medical Clinics of North America* **22**, 453-476 (1978).
- 7 Peng, X. *et al.* Transmission routes of 2019-nCoV and controls in dental practice. *International Journal of Oral Science* **12**, 9, doi:10.1038/s41368-020-0075-9 (2020).
- 8 Epstein, J. B., Chow, K. & Mathias, R. Dental procedure aerosols and COVID-19. *The Lancet Infectious Diseases*, doi:[https://doi.org/10.1016/S1473-3099\(20\)30636-8](https://doi.org/10.1016/S1473-3099(20)30636-8) (2020).
- 9 Ge, Z. Y., Yang, L. M., Xia, J. J., Fu, X. H. & Zhang, Y. Z. Possible aerosol transmission of COVID-19 and special precautions in dentistry. *J Zhejiang Univ Sci B* **21**, 361-368, doi:10.1631/jzus.B2010010 (2020).
- 10 Milton, D. K., Fabian, M. P., Cowling, B. J., Grantham, M. L. & McDevitt, J. J. Influenza virus aerosols in human exhaled breath: particle size, culturability, and effect of surgical masks. *PLoS Pathog* **9**, e1003205, doi:10.1371/journal.ppat.1003205 (2013).
- 11 Rautemaa, R., Nordberg, A., Wuolijoki-Saaristo, K. & Meurman, J. H. Bacterial aerosols in dental practice - a potential hospital infection problem? *J Hosp Infect* **64**, 76-81, doi:10.1016/j.jhin.2006.04.011 (2006).
- 12 Veena, H. R., Mahantesha, S., Joseph, P. A., Patil, S. R. & Patil, S. H. Dissemination of aerosol and splatter during ultrasonic scaling: A pilot study. *Journal of Infection and Public Health* **8**, 260-265, doi:<https://doi.org/10.1016/j.jiph.2014.11.004> (2015).
- 13 Sachdev, R., Garg, K., Singh, G. & Mehrotra, V. Is safeguard compromised? Surgical mouth mask harboring hazardous microorganisms in dental practice. *J Family Med Prim Care* **9**, 759-763, doi:10.4103/jfmpc.jfmpc_1039_19 (2020).
- 14 Hallier, C., Williams, D. W., Potts, A. J. & Lewis, M. A. A pilot study of bioaerosol reduction using an air cleaning system during dental procedures. *Br Dent J* **209**, E14, doi:10.1038/sj.bdj.2010.975 (2010).
- 15 Mupparapu, M. & Kothari, K. R. M. Review of surface disinfection protocols in dentistry: a 2019 update. *Quintessence Int* **50**, 58-65, doi:10.3290/j.qi.a41337 (2019).
- 16 Sawhney, A. *et al.* Aerosols how dangerous they are in clinical practice. *J Clin Diagn Res* **9**, ZC52-57, doi:10.7860/JCDR/2015/12038.5835 (2015).

- 17 Joshi, A. A., Padhye, A. M. & Gupta, H. S. Efficacy of Two Pre-Procedural Rinses at Two Different Temperatures in Reducing Aerosol Contamination Produced During Ultrasonic Scaling in a Dental Set-up - A Microbiological Study. *J Int Acad Periodontol* **19**, 138-144 (2017).
- 18 Teanpaisan, R., Taeporamaysamai, M., Rattanachone, P., Poldoung, N. & Srisintorn, S. The usefulness of the modified extra-oral vacuum aspirator (EOVA) from household vacuum cleaner in reducing bacteria in dental aerosols. *Int. Dent. J.* **51**, 413-416, doi:10.1002/j.1875-595X.2001.tb00853.x (2001).
- 19 Noro, A. *et al.* A study on prevention of hospital infection control caused by tooth preparation dust in the dental clinic. Part 1. Preventive measures against environmental pollution in the dental clinic caused by microbial particles. *Bull Tokyo Dent Coll* **36**, 201-206 (1995).
- 20 Zhao, B., An, N. & Chen, C. Using air purifier as a supplementary protective measure in dental clinics during the COVID-19 pandemic. *Infect. Control Hosp. Epidemiol.*, 1-4, doi:10.1017/ice.2020.292 (2020).
- 21 Hubar, J. S., Pelon, W., Strother, E. A. & Sicard, F. S. Reducing Staphylococcus aureus bacterial counts in a dental clinic using an Ionic Breeze air purifier: a preliminary study. *Gen Dent* **57**, 226-229 (2009).
- 22 Lin, Y. *et al.* Probing the structure of the SARS coronavirus using scanning electron microscopy. *Antivir Ther* **9**, 287-289 (2004).
- 23 Davies, M. H., Rosen, M., Eccles, J. D. & Marshal, R. J. Criteria of air flow and negative pressure for high volume dental suction. *Br. Dent. J.* **130**, 483-487, doi:10.1038/sj.bdj.4802680 (1971).
- 24 Programme, S. D. C. E. *Mitigation of AGPs in Dentistry, A rapid review*. Vol. 1.0.25 (2020).
- 25 R Holliday, J. A., CC Currie, DC Edwards, C Bowes, K & Pickering , S. R., J Durham, N Rostami, J Coulter, N Jakubovics. Evaluating dental aerosol and splatter in an open plan clinic environment: implications for the COVID-19 pandemic. <https://doi.org/10.31219/osf.io/md49f> (2020).
- 26 Bourouiba, L. Turbulent Gas Clouds and Respiratory Pathogen Emissions: Potential Implications for Reducing Transmission of COVID-19. *JAMA* **323**, 1837-1838, doi:10.1001/jama.2020.4756 (2020).

Supplementary data

ANNEX A: Influence of silicone tubing on particle distribution measurements

Materials and Methods

Sodium chloride (>95%) was purchased from Fisher Scientific, Leicestershire, UK. Ultra-pure water (>18.2 M Ω) was obtained by ultrafiltration of the municipal supply via a MilliQ Integral 3 (Millipore, MA, USA). Silicone tubing (“Tygon[®]”) was purchased from the Cole-Parmer Instrument Co (Illinois, USA) and was reported to have the following dimensions: internal diameter 12.7 mm, outer diameter 17.5 mm, wall thickness 2.4 mm). The tubing was cut into 6 x 2m sections.

The Study was performed in a custom-built chamber (internal dimensions 7.6 m (h) x 4.6 m x 4.6 m; volume $\sim 160.8 \text{ m}^3$) lined with a chemically resistant epoxy resin (Renotex Rollercoat, Renotex Ltd, Wakefield, UK) with a powder-coated, glass-reinforced plastic floor suspended at a height of 1 m from the base of the chamber. The chamber environment was maintained at constant temperature and humidity ($21 \pm 1^\circ \text{C}$, $40 \pm 2 \% \text{RH}$) through an internally mounted air conditioning unit (iQool12, Aircon Direct, UK). Air was removed from the chamber via a stainless steel central duct ($\phi = 150 \text{ mm}$; wind velocity at orifice $\sim 3.15 \text{ m s}^{-1}$) below the suspended floor and was recirculated via five, overhead polypropylene ducts ($\phi = 110 \text{ mm}$; velocity $\sim 1.6 \text{ ms}^{-1}$ at each duct orifice) suspended 0.2 m below the chamber ceiling. The recirculation rate was controlled by an in-line, variable speed pump (Model DV150, P&G Fabrications, Essex, UK). Air within the chamber was agitated using a metal-bladed electric fan (model W4E400-DS02-38, RS Components, UK) which produced a constant air speed of $\sim 1.5 \text{ m s}^{-1}$ at a distance of 1.5 m. Entry to the exposure chamber was via an air-lock, operating at an over pressure of $\sim 5 \text{ mBar}$.

The aerosol was produced using a spray gun (DeVilbliss Cobra 1 automatic spray gun, Hitech Spray Ltd, UK) fitted with fluid nozzle and separator (SP-200S-12-K, Devilbliss) and air cap (SP-100-522-COM-K, Devilbliss), with a 2.27 L pressure kettle (DeVilbliss KBII, Hitech Spray Ltd, UK; operating pressure 2.5 PSI) containing 20% (w/w) aqueous sodium chloride. Compressed air (90 PSI) was supplied from a compressor (ABAC Aria Compressa S.p.A., Model B 2800B, Robassomero, Italy). The output from the spray gun was directed through an impactor (comprising 1.2 m length of 10 mm diameter steel ducting bent through 180°) to remove large ($>10 \mu\text{m}$) particles. A small ($\phi = 8 \text{ mm}$) vent was placed at the base of the impactor to drain excess fluid ($\sim 20\%$ of the initial injection volume). Aerosol was generated within the chamber until the total particle concentration was $2.11 \pm 0.16 \times 10^6 \text{ cm}^{-3}$. The particle concentration and corresponding aerosol size distribution was measured using a high-resolution particle sizer (ELPI+, Dekati, Kangasala, Finland) at a sample acquisition rate of 1 Hz.

The study started with a 30 s baseline aerosol measurement by the particle sizer, after which the first silicone tube was attached to the particle sizer for a further 30 s period. The tube was then disconnected for 30 seconds and the process repeated three times before the tubing

was changed (see study design; Figure 1). Each tube was positioned so that it was curved at the proximal and distal ends (Figure 2).

Figure S1: Outline study design indicating connection to particle sizer.

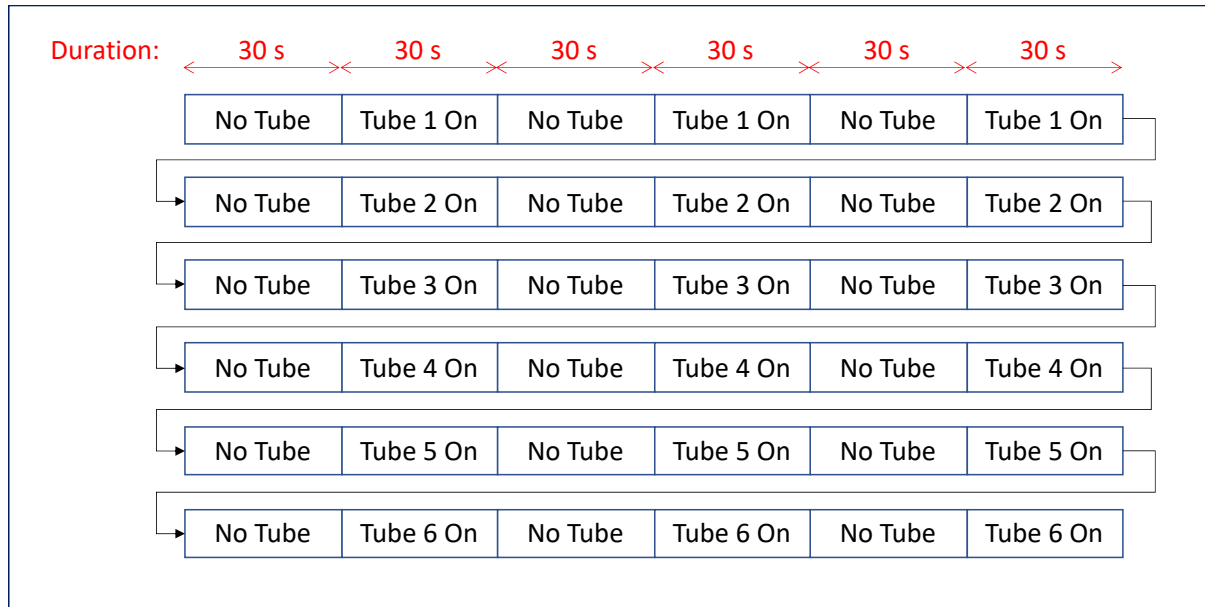


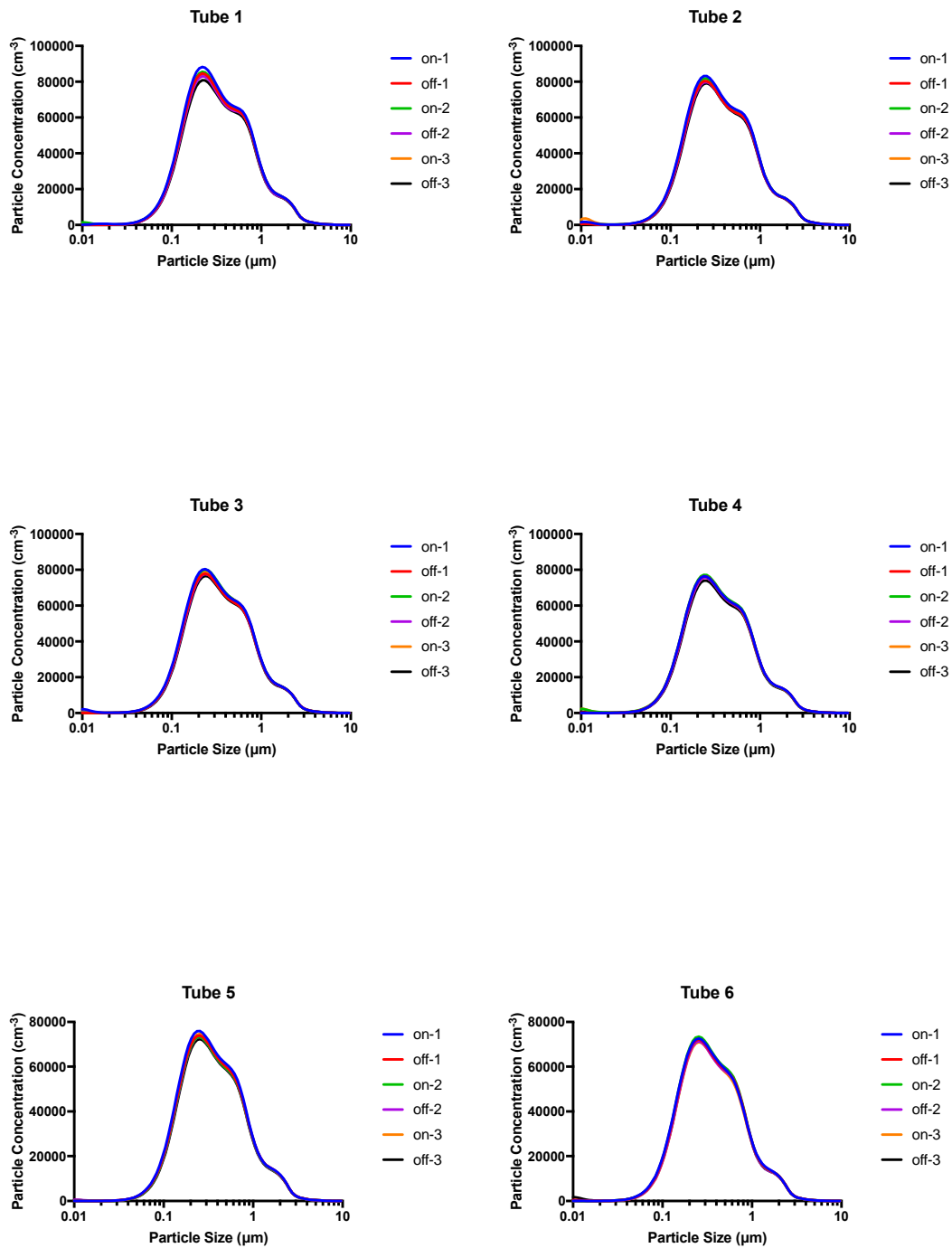
Figure S2: Position of silicone tube relative to the particle sizer.



Results

Triplicate cycles of connecting and disconnecting each tube had no observable effect on the measured particle size distribution (Figure S3).

Figure S3: Particle size distribution of salt aerosol measured in the presence (“on”) or absence (“off”) of tubes 1 – 6. Each tube was connected/disconnected in three cycles (1-3).



ANNEX B: Particle distribution histograms

Figure S4: Particle size distributions measured at Location 3 under treatment A (Control) during procedures I to VI and at the end of the Decay period.

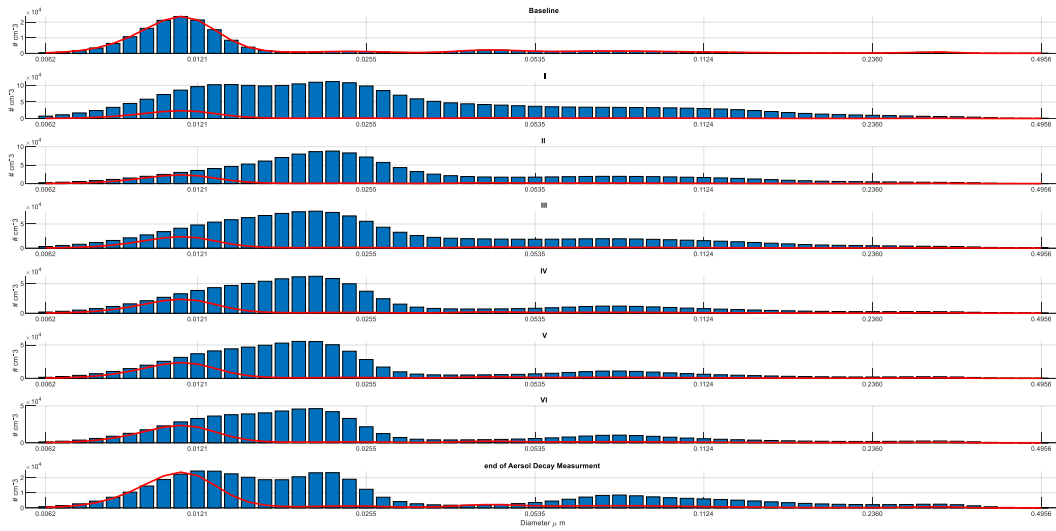
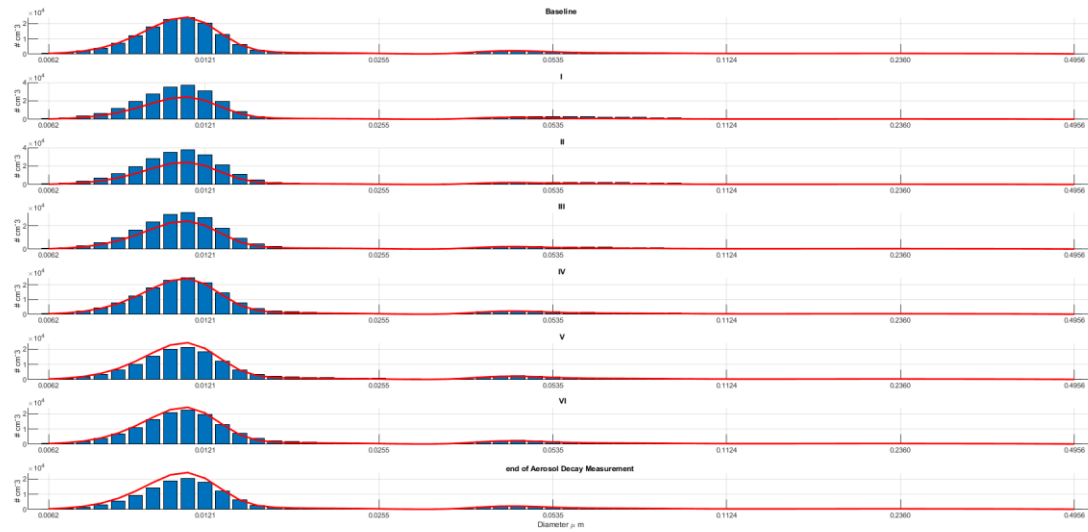
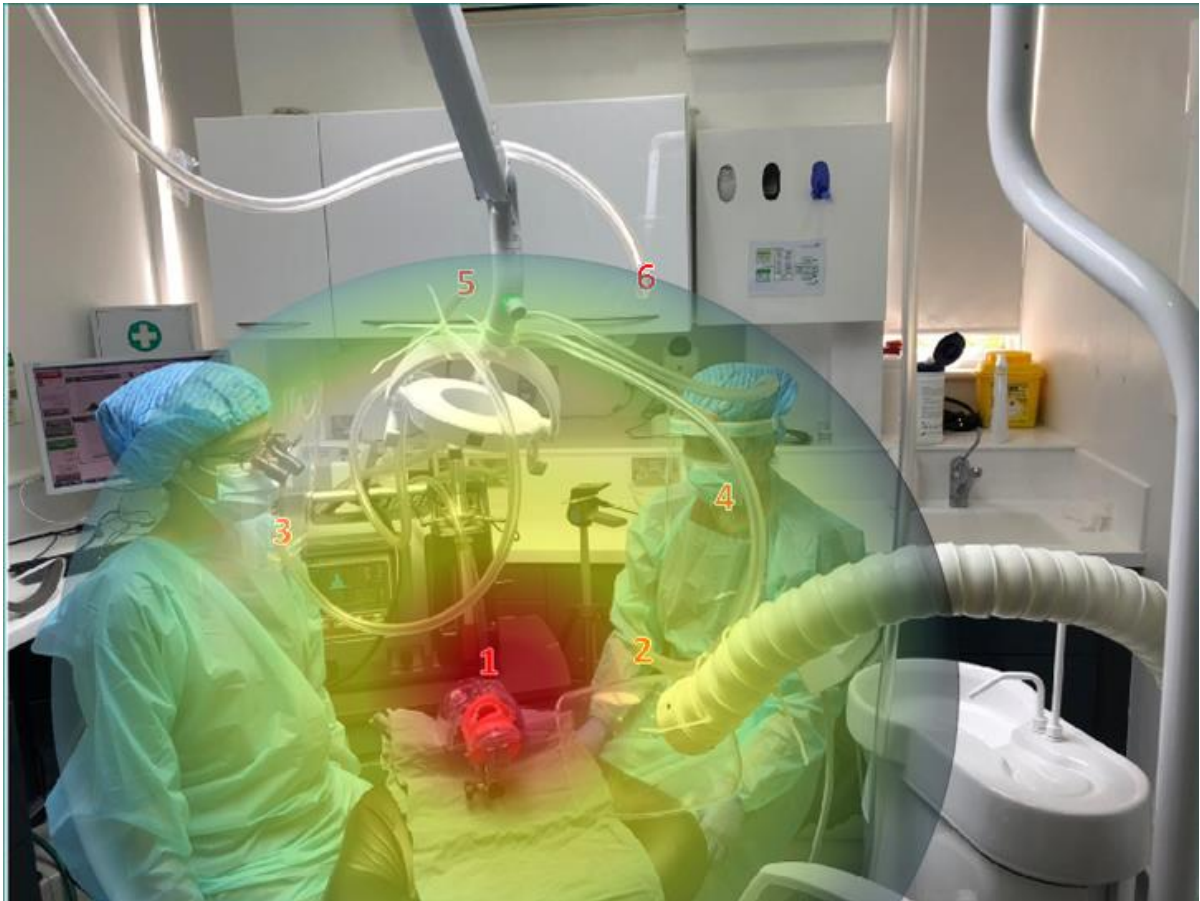


Figure S5: Particle size distributions measured at Location 3 under treatment E (HVS(IO) + HVS (EO) + ACS) during procedures I to VI and at the end of the Decay period.



ANNEX C: Micro and macro environments

Figure S6: Diagram presenting the aerosol dispersion envelopes in a dental clinic. Red and yellow zone show the micro-environment with the highest aerosol concentration. The blue shading represents the interface between micro and macro environment, where lower aerosol concentrations were measured.



ANNEX D: Supplementary Figures

Figure S7: Total particle concentration generated during AGPs in the presence of HVS(10) (treatment group B; Table 2) at each air sampling location (1 – 6; Table 1). Acquisition of air samples were performed during the baseline period (0 – 3 min), during the six procedures (3 – 18 min) and following cessation of procedures (18 – 36 min). Dotted lines indicate the upper and lower boundaries of the baseline data. Each data point represents the sum of particles measured by HR-ELPI over 1 second during each replicate (n=3).

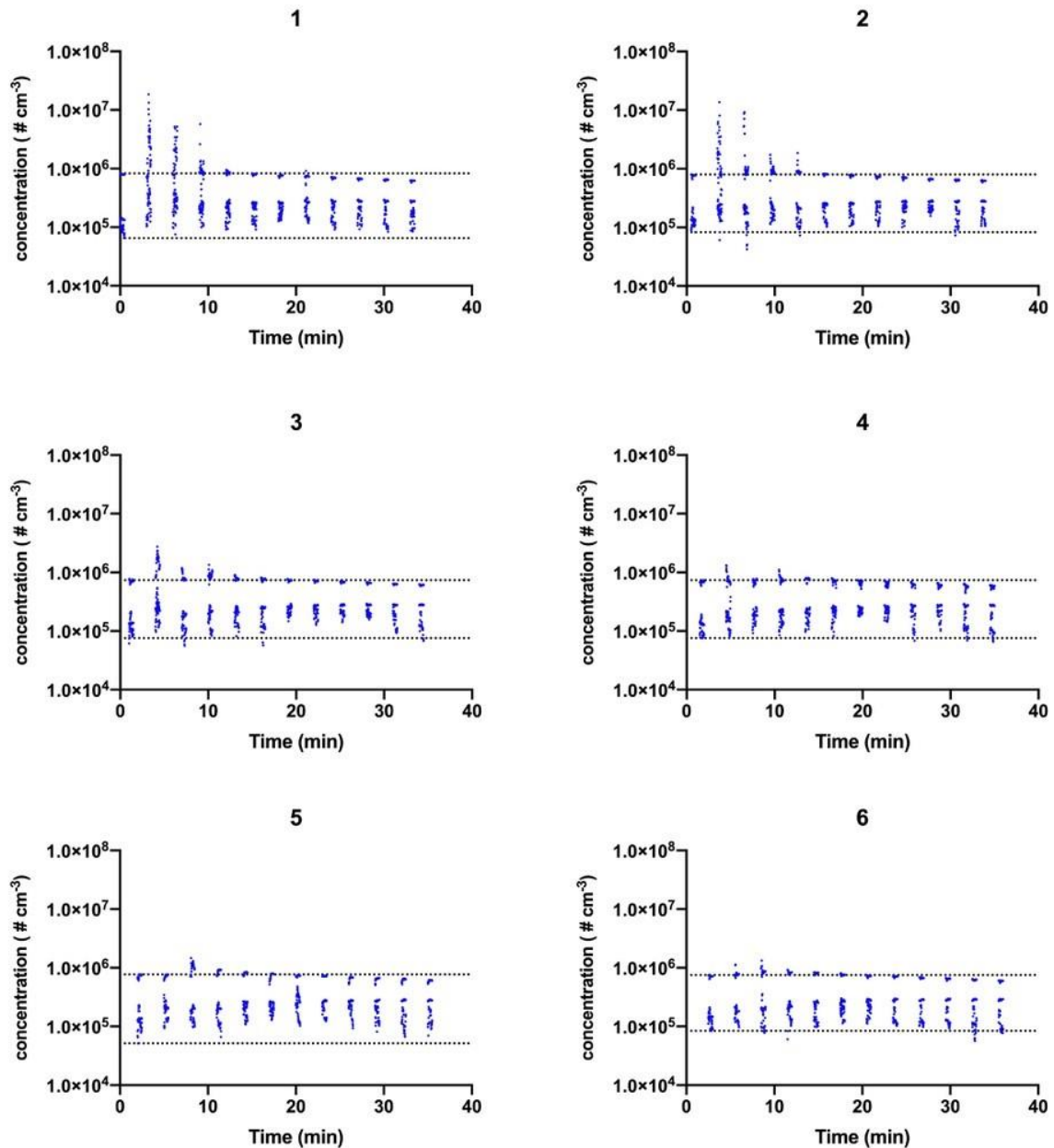


Figure S8: Total particle concentration generated during AGPs in the presence of HVS(IO) and ACS (treatment group C; Table 2) at each air sampling location (1 – 6; Table 1). Acquisition of air samples were performed during the baseline period (0 – 3 min), during the six procedures (3 – 18 min) and following cessation of procedures (18 – 36 min). Dotted lines indicate the upper and lower boundaries of the baseline data. Each data point represents the sum of particles measured by HR-ELPI over 1 second during each replicate (n=3).

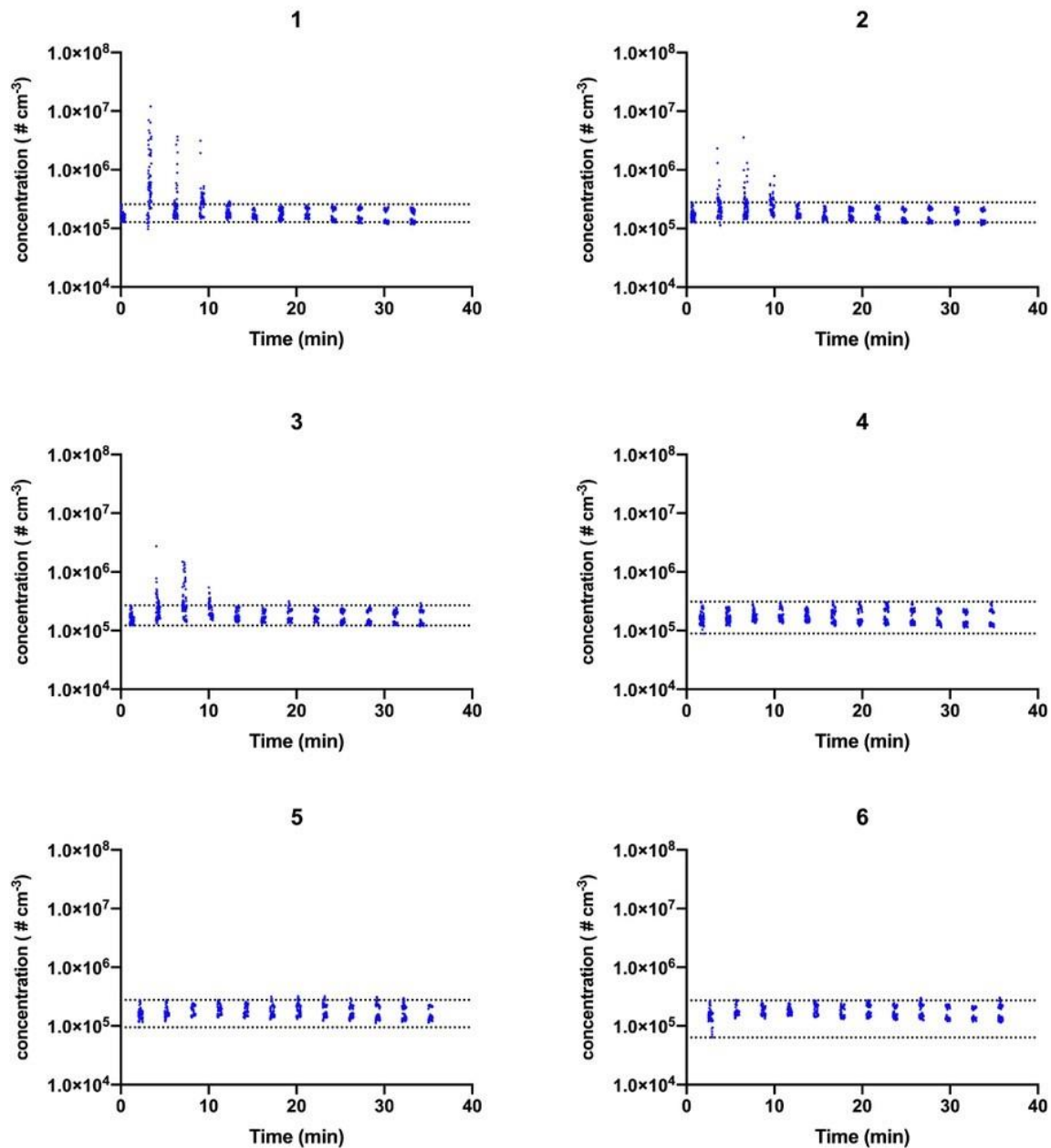


Figure S9: Total particle concentration generated during AGPs in the presence of HVS(IO) and HVS(EO) (treatment group D; Table 2) at each air sampling location (1 – 6; Table 1). Acquisition of air samples were performed during the baseline period (0 – 3 min), during the six procedures (3 – 18 min) and following cessation of procedures (18 – 36 min). Dotted lines indicate the upper and lower boundaries of the baseline data. Each data point represents the sum of particles measured by HR-ELPI over 1 second during each replicate (n=3).

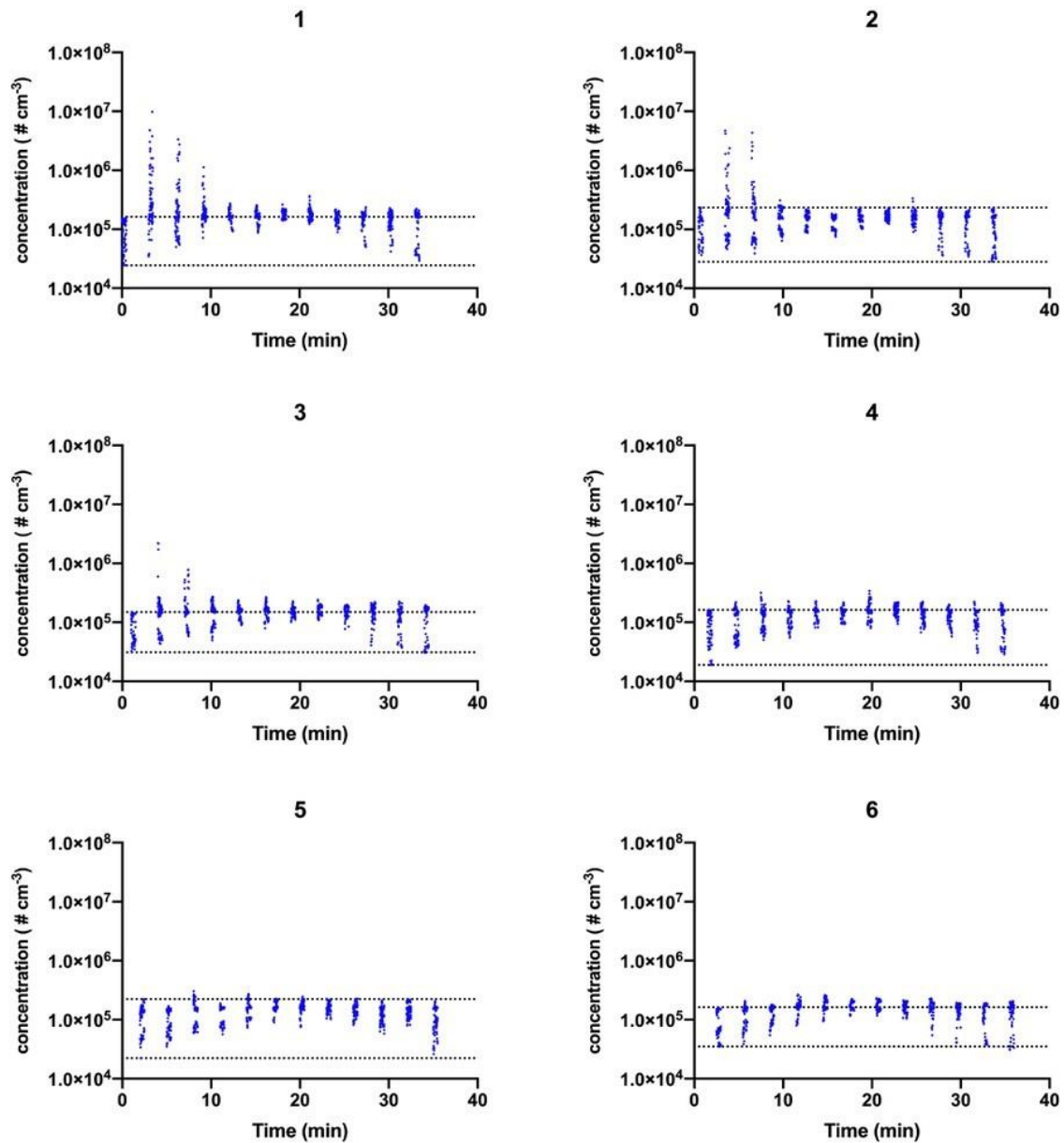
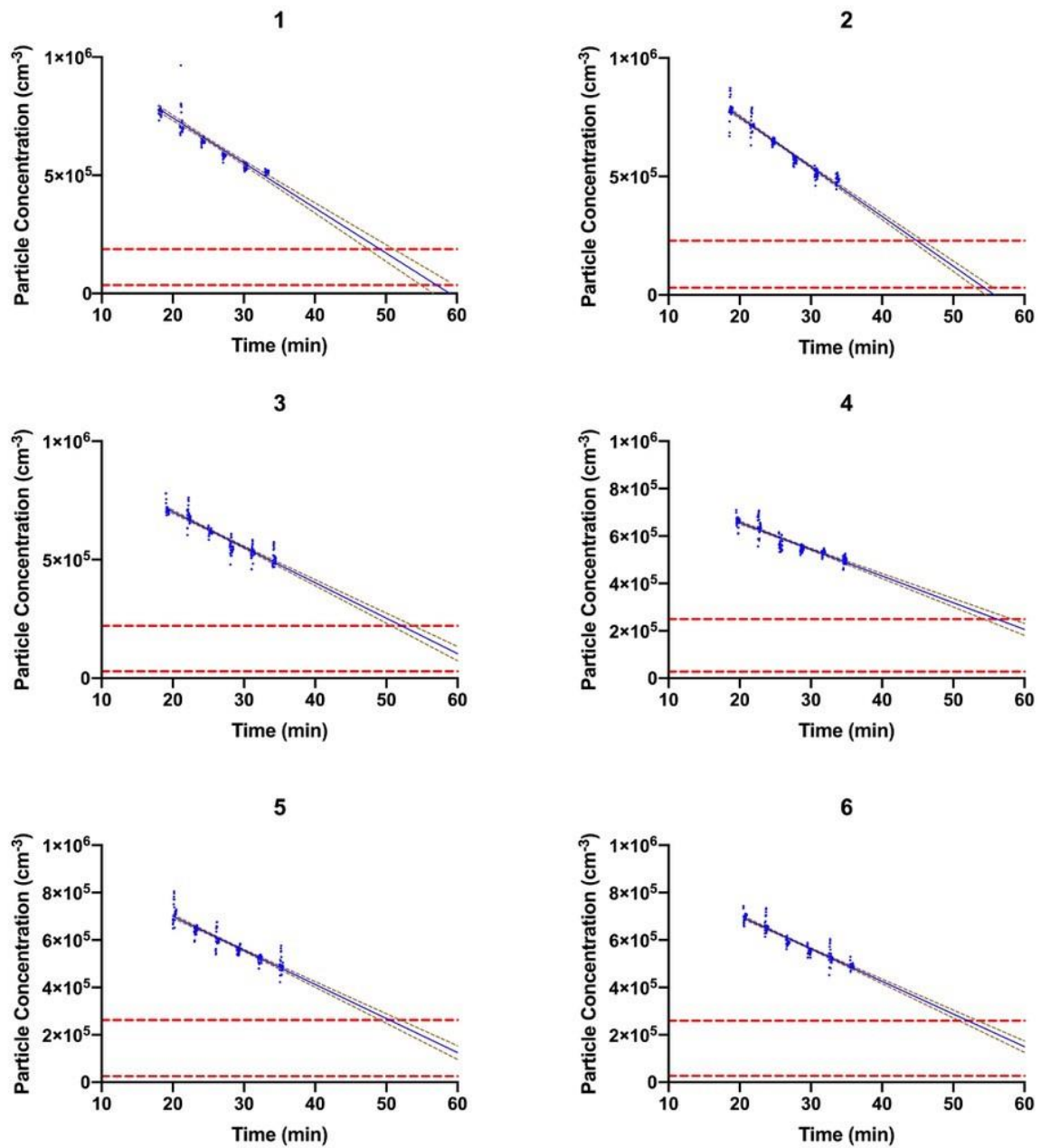


Figure S10: Linear regression (with 95% confidence intervals) of decay-phase particle concentration data. Each data point represents the median sum particle concentration measured by HR-ELPI per second during each replicate (n=3). Dotted line indicates baseline particle range.



Regression parameter	Location					
	1	2	3	4	5	6
Y-Intercept	1.1E+06	1.2E+06	1.0E+06	8.8E+05	9.9E+05	9.8E+05
Slope	-1.9E+04	-2.1E+04	-1.5E+04	-1.1E+04	-1.4E+04	-1.4E+04
r ²	0.7967	0.9218	0.8609	0.8273	0.8533	0.8827

D: Supplementary Tables

Table S1: Air sampling location coordinates, expressed relative to the phantom head (nominal coordinates $x=0$, $y=0$, $z=0$).

Sample Location No.	Name	Co-ordinates relative to phantom head (mm)			Linear Distance from source (mm)
		x	y	z	
1	Phantom head (source)	0	80	0	80
2	HVS (EO) in-take	135	-110	100	200
3	Dentist	-262	145	265	400
4	Assistant	354	160	300	500
5	Wall	0	900	1045	1480
6	Light	726	383	1495	1700

Table S2: Summary of aerosol removal treatments used in each experiment. Note that intra-oral low volume suction (LVS) was used in all treatment groups (including control) to represent standard practice and to prevent excess fluid accumulation within the phantom head.

	Interventions			
	LVS Low volume suction	HVS(IO) High Volume Suction (Intra-oral) with air filtration system.	HVS(EO) High Volume Suction (extra-oral).	ACS Air Cleaning System.
Intervention group				
A	X			
B	X	X		
C	X	X		X
D	X	X	X	
E	X	X	X	X

Table S3: Procedural equipment and corresponding coolant flow rates.

Procedure	Description	Coolant Flow Rate (mL min⁻¹)
I	W&H Synea Vision TK94 hand-piece (Air Turbine) with long tapered bur	55
II	NSK Ti Max Z95L hand piece (Electric) with long tapered bur	67
III	Sirona T1 Control hand-piece (Air turbine) with long tapered bur	56
IV	3 in1 syringe from Belmont Cleo II chair	82
V	Cavitron Jet Plus Ultrasonic with 30K FSI-SLI tip	25
VI	NSK Vario Lux 2 (Piezo) with G8 tip	78